Supplementary Information for

Enhancement of Long Stability of Li-S battery by Thin Wall Hollow Spherical Structured Polypyrrole Based Sulfur Cathode

Guoqiang Ma, Zhaoyin Wen*, Jun Jin, Yan Lu , Xiangwei Wu, Cai Liu, Chunhua Chen

The design process of T-HSSP

Firstly, the sulfur content in the S@PPy composite is designed as 60%, and not all the sulfur is encapsulated into the holes of HSPS, maybe 30% of sulfur is deposited on the outer surface of T-HSSP or the other position. The thickness of the shell should be as less as 30nm.

As known,

Density of S: $\rho_S = 2$ g/cm^3.

Density of PPy: $\rho_{PPy} = 1$ g/cm^3.

So the volume of sulfur in the holes 1g T-HSSP is:

$$1g \times \frac{60\%}{1-60\%} \times (1-30\%) \div 2g/cm^3 = 0.525\text{cm}^3$$

The volume expansion is as high as 80%. So the void space for 1g T-HSSP should be:

$(1+80\%) \times 0.525\text{cm}^3 = 0.945\text{cm}^3$

The thickness of T-HSSP should be as less as 30nm to ensure the mechanical performance of hollow sphere.

The diameter of the T-HSSP is assumed as: D

D is calculated according to the equation as follows:

$$\frac{(D-60)m^3}{Dnm^3-(D-60)nm^3} \times \frac{1}{1g/cm^3} \geq 0.945\text{cm}^3/\text{g}$$

D>280nm

Therefore, the diameter of the T-HSSP is determined as **300**nm.

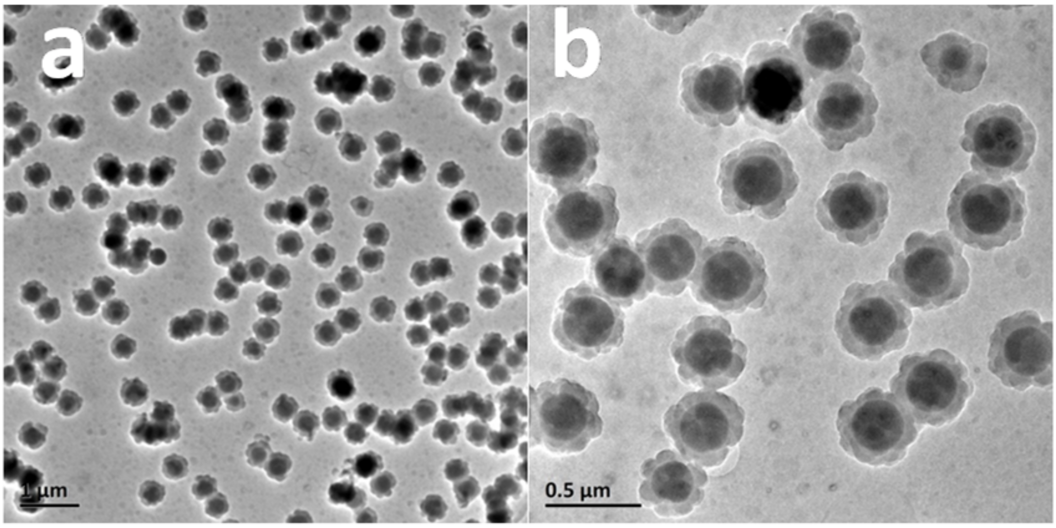

Supplementary Figure. S1. TEM images of the PPy@SiO$_2$ composite.

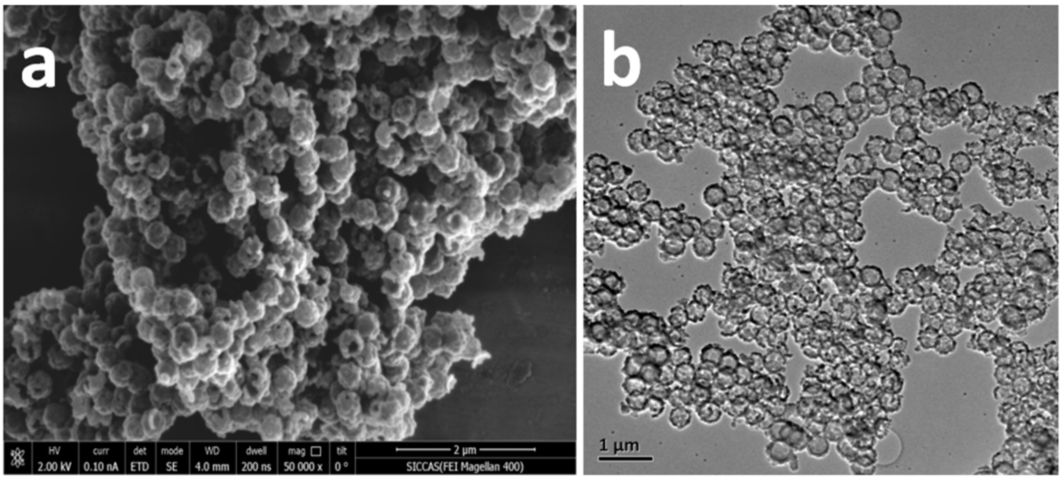

Supplementary Figure. S2. The SEM images of the T-HSSP.

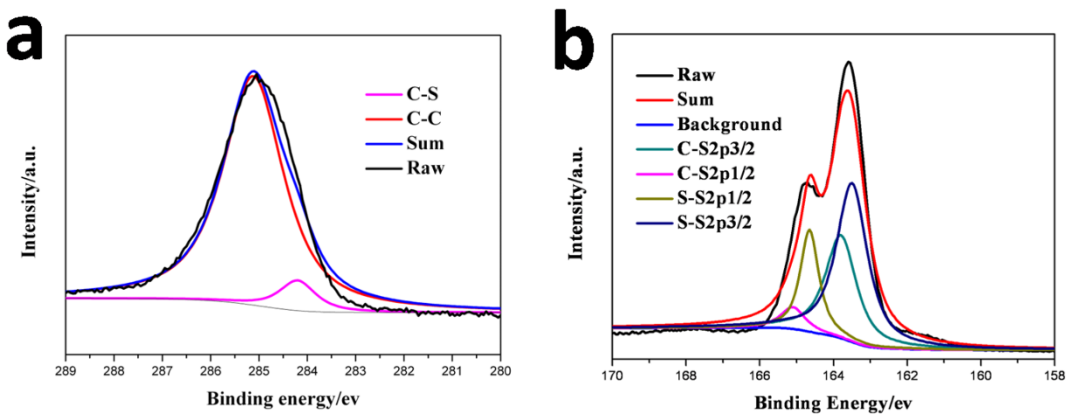

Supplementary Figure. S3. XPS spectra of the S@PPy-300 composite in C 1s region (a), and S 2p region (b).

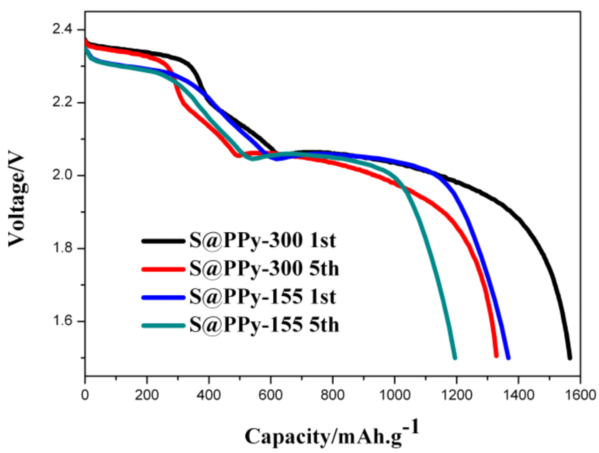

Supplementary Figure. S4. The discharge profiles of S@PPy-155 and S@PPy-300 at 1st cycle and 5th cycle. As seen, the discharge profiles of S@PPy-155 is similar to those of the common S/C cathode. While there is another plateau between 2.3V and 2.0V, which corresponds to the existence of S-C bond in S@PPy-300 sample.

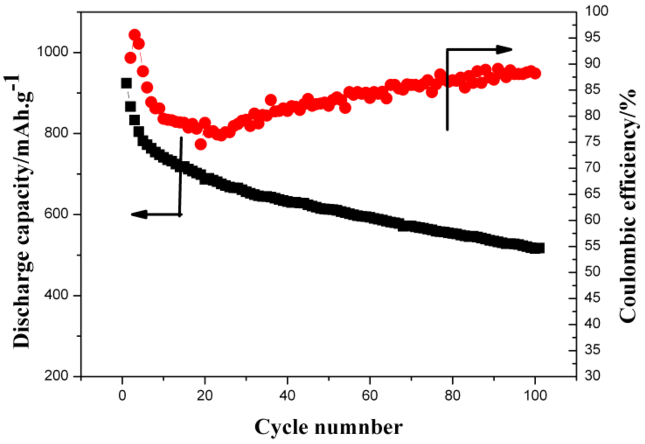

Supplementary Figure.S5. The cycling performance and coulombic efficiencies of pure sulfur cathode. As seen, the cycling stability of pure sulfur cathode is much worse than that of S@PPy-300 sample, thus the enhanced cycling performance is attributed to the designed sulfur cathode. And the coulombic efficiencies is lower than those of S@PPy-300, showing shuttle effect is suppressed evidently by the designed sulfur cathode.

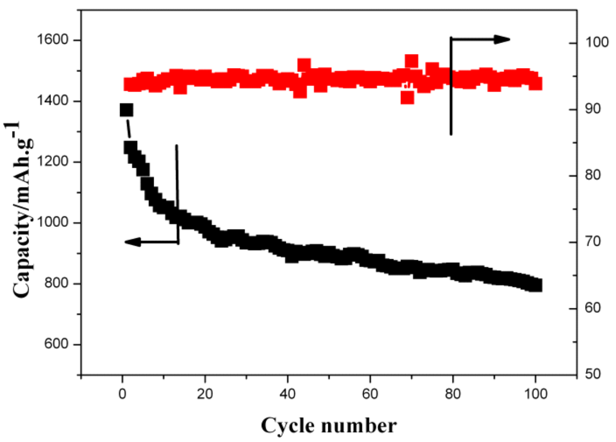

Supplementary Figure.S6. The cycling performance of S@PPy-155 cathode. The initial discharge capacity of S@PPy-155 is lower than that of S@PPy-300, indicating a more uniform distribution of sulfur in the cathode is obtained under higher heating treatment temperature. Moreover, the cycling stability of S@PPy-300 is better than that of S@PPy-155, which is attributed to the more uniform distribution of sulfur in the cathode and C-S bond generated during higher heating treatment temperature.

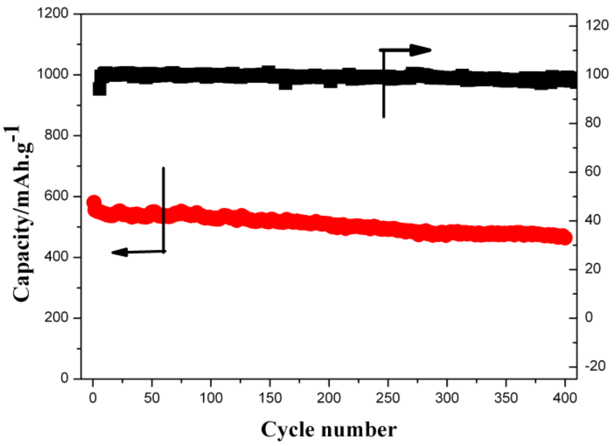

Supplementary Figure.S7. The cycling performance of H-S@PPy sulfur cathode at 5C. The sulfur on the outer surface of T-HSSP is removed by a heating treatment process. Thus the cycling performance of Li-S battery is further enhanced, the severe capacity fade in the initial tens of cycles is inhibited effectively.

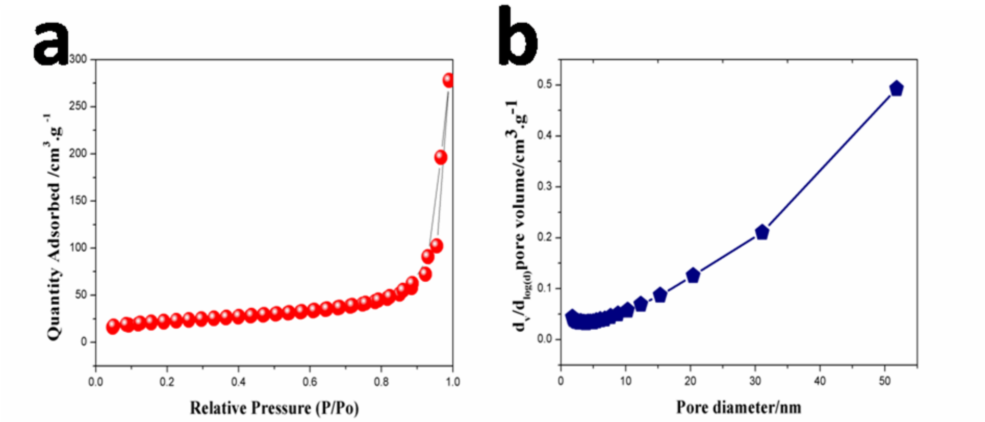

Supplementary Figure. S8. (a) N_2 adsorption/desorption isotherm, (b) pore size distribution of the PPy hollow sphere. The big specific surface (109m^2/g) and the pore volume of the pores (0.43cm^3/g) can be attributed to that the PPy hollow spheres are composed of PPy nano-particles.